1-1-2012

Numerical analysis of bearing reinforcement earth (BRE) wall

Cherdsak Suksiripattanapong
Suranaree University of Technology Thailand

Avirut Chinkulkijniwat
Suranaree University of Technology

Suksun Horpibulsuk
Suranaree University of Tech, Thailand, suksun@g.sut.ac.th

Cholachat Rujikiatkamjorn
University of Wollongong, cholacha@uow.edu.au

Theerasak Tanhsutthinon
Geoform Co., Ltd

NUMERICAL ANALYSIS OF BEARING REINFORCEMENT EARTH (BRE) WALL

Cherdsak Suksiripattanapong, B.Eng.(Hons), M.Eng.
Ph.D. Scholar, School of Civil Engineering,
Suranaree University of Technology,
111 University Avenue, Muang District,
Nakhon Ratchasima 30000, THAILAND

Avirut Chinkulkijniwat, B.Eng.(Hons), M.Eng., Ph.D.
Assistant Professor, School of Civil Engineering,
Suranaree University of Technology,
111 University Avenue, Muang District,
Nakhon Ratchasima 30000, THAILAND

Suksun Horpibulsuk, B.Eng.(Hons), M.Eng., Ph.D.
Professor and Chair, School of Civil Engineering,
Head, Construction Technology Research Unit,
Suranaree University of Technology,
111 University Avenue, Muang District,
Nakhon Ratchasima 30000, THAILAND
Tel: +66-44-22-4322 and +66-89-767-5759, Fax: +66-44-22-4607
Email: suksun@g.sut.ac.th and suksun@yahoo.com

Cholachat Rujikiatkamjorn, B.Eng.(Hons), M.Eng., Ph.D.
Senior Lecturer, Civil Engineering Division,
Faculty of Engineering, University of Wollongong,
Wollongong City, NSW 2522, AUSTRALIA

Theerasak Tangsutthinon, B.Sc. (Geology)
General Manager, Geoform Co., Ltd.
Bangkok 10900, THAILAND

Date written: 26 December 2011
Number of words: 4,857

NOTE: The third author is the corresponding author. Mail communication may please be addressed to Dr. Suksun Horpibulsuk, School of Civil Engineering, Suranaree University of Technology, 111 University Avenue, Muang District, Nakhon Ratchasima 30000, THAILAND

NUMERICAL ANALYSIS OF BEARING REINFORCEMENT EARTH (BRE) WALL

Cherdsak Suksiripattanapong[1], Avirut Chinkulkijniwat[2], Suksun Horpibulsuk[3*], Cholachat Rujikiatkamjorn[4] and Theerasak Tanhsutthinon[5]

[1, 2, 3] School of Civil Engineering, Suranaree University of Technology, Nakhon Ratchasima, 30000, Email: suksun@g.sut.ac.th
[4] Senior Lecturer, Centre for Geomechanics and Railway Engineering, Civil Engineering Division, Faculty of Engineering, University of Wollongong, Wollongong City, NSW 2522, Australia
[5] General Manager, Geoform Co. Ltd., Thailand

ABSTRACT: This paper presents a numerical simulation of the bearing reinforcement earth wall by PLAXIS 2D. The bearing reinforcement was regarded as a cost-effective earth reinforcement. The model parameters for the simulation were obtained from the conventional laboratory tests and back analyses from the laboratory pullout tests of the bearing reinforcement. The simplified method for modeling the bearing reinforcement, which converts the contribution of friction and bearing resistance to the equivalent friction resistance, is introduced. This method is considered to be acceptable and practical in working state with sufficient factor of safety and small pullout displacement. The bearing reinforcement is modeled as the geotextile and the equivalent friction resistance is represented by the soil/reinforcement interface parameter, *R*, which was obtained from a back analysis of the laboratory pullout test results. The *R* values are 0.65 and 0.75 for the bearing reinforcement with 2 and 3 transverse members, respectively. The change in bearing stresses, settlements, lateral earth pressures and tensions in the reinforcements during and after construction is simulated. Overall, the simulated test results are in good agreement with the measured ones. The simulated results show that the BRE wall behaves as a rigid body, retaining the unreinforced backfill. The simulated bearing stress presents a trapezoid distribution shape as generally assumed by the conventional method of examination of the

external stability of MSE walls. The simulated settlement is almost uniform due to a high stiffness of the rigid foundation and the bearing reinforcements. The maximum lateral movement occurs at about the mid-height of the wall, resulting in the bi-linear maximum tension plane. The knowledge gained from this study can be applied to other BRE walls with different wall heights, foundations and features of bearing reinforcements.

KEYWORDS: bearing reinforcement, finite element analysis, mechanically stabilized earth wall

1. INTRODUCTION

The use of inextensible reinforcements to stabilize earth structures has grown rapidly in the past two decades. When applied for retaining walls or steep slopes, they can be laid continuously along the width of the reinforced soil system (grid type) or laid at intervals (strip type). Both grid and strip reinforcements are widely employed around the world, including Thailand and Australia. The construction cost of the mechanically stabilized earth (MSE) wall is mainly dependent upon the transportation of backfill from a suitable borrow pit and the reinforcement type. The backfill is generally granular materials. The transportation of the backfill is thus a fixed cost for a particular construction site. Consequently, the reinforcement becomes the key factor, controlling the construction cost for a particular site.

Horpibulsuk and Niramitkornburee (2010) have introduced a cost-effective earth reinforcement designated as “Bearing reinforcement”. It is simply installed, conveniently transported and possesses high pullout and rupture resistances with less steel volume. Figure 1 shows the typical configuration of the bearing reinforcement, which is composed of a longitudinal member and transverse (bearing) members. The longitudinal member is a steel deformed bar and the transverse members are a set of steel equal angles. This reinforcement has been introduced into practice in Thailand since 2008 by the Geoform Co., Ltd. Several earth walls stabilized with the bearing reinforcements were constructed at various parts of Thailand. This reinforcement has been considered to be one of the standard earth reinforcements for the Department of Highways, Thailand. The earth wall stabilized by the bearing reinforcements is designated as “bearing reinforcement earth (BRE) wall”.

Figure 1: Configuration of the bearing reinforcement (Horpibulsuk and Niramitkornburee, 2010).

For a MSE wall design, an examination of external and internal stability is a routine design procedure. The examination of external stability is generally performed using the conventional method (limit equilibrium analysis) assuming that the composite backfill-reinforcement mass behaves as a rigid body (McGown et al., 1998). The external stability of the BRE wall with the vertical spacing of the reinforcement less than 750 mm was successfully examined by the conventional method (Horpibulsuk et al., 2010 and 2011). The internal stability of the BRE wall deals with the rupture and pullout resistances of the reinforcement. The practical equations for estimating pullout resistance of the bearing reinforcement with different transverse members were proposed by Horpibulsuk and Niramitkornburee (2010). The equations were successfully used to design the BRE wall in Thailand. To verify the concept, a full-scale test BRE wall was designed by the limit equilibrium analysis and constructed in the campus of Suranaree University of Technology (Horpibulsuk et al., 2010 and 2011). The performance of the BRE wall was measured and reported. The small lateral movement and settlement were observed. The practical method of designing the BRE found on the hard stratum was introduced. This method has been adopted to design several BRE walls under the Department of Highways, Thailand.

The performance of MSE walls was extensively studied using the full-scale, laboratory model tests and numerical simulation (Bergado et al., 2000; Bergado and Teerawattanasuk, 2007; Park and Tan, 2005; Skinner and Rowe, 2005; Al Hattamleh and Muhunthan, 2006; Hatami and Bathurst, 2005 and 2006; and Abdelouhab et al., 2011). The PLAXIS program has been proved as a powerful and precise tool for predicting the performance of the MSE wall and pullout test results (Bergado et al., 2003; and Khedkar and Mandal, 2007 and 2009). This paper presents a numerical simulation of the performance of the BRE wall during and after construction, which includes settlement, bearing stress, lateral movement, lateral earth pressure and tension force in the reinforcements. The full-scale test

results by Horpibulsuk et al. (2011) were taken for this simulation. The simulation was performed using the finite element code (PLAXIS 2D). The bearing reinforcement was modeled as the geotextile with an equivalent friction resistance. The equivalent friction resistance is represented by the soil/reinforcement interface parameter and was obtained from the back analysis of the laboratory pullout test results. The other model parameters were obtained from the conventional laboratory tests. The knowledge gained from this simulation provides a useful information for further analysis and design of the other BRE walls with different wall heights, ground conditions and features of bearing reinforcement.

2. FULL SCALE TEST OF BEARING REINFORCEMENT EARTH (BRE) WALL

2.1 Subsoil investigation

A full-scale test on a bearing reinforcement earth wall was performed at the campus of Suranaree University of Technology (SUT) on 20 July 2009. The general soil profile consisted of weathered crust layer of silty sand over the top 1.5 m. This layer was underlain by medium dense silty sand down to about 6 m depth. Below the medium dense sand layer was the very dense silty sand. The ground water was not observed even up to 8 meter depth (end of boring). Figure 2 shows the soil profile of the site. The in-situ strength of the subsoil was measured using the standard penetration test.

Figure 2: General soil profile

2.2 Feature of the test Bearing Reinforcement Earth Wall

The wall was 6 m high, 9 m long and 6 m wide at the top, and 21 m long and 12 m wide at the base, as illustrated in Figures 3 and 4. The side and back slopes were 1:1. The

BRE wall was designed based on the limit equilibrium analysis. The detailed design was explained elsewhere by Horpibulsuk et al. (2010 and 2011). The ground was first excavated to 0.5 m depth below the original ground where the wall base was located. The wall facing panels were placed on a lean concrete leveling pad (0.15 m width and 0.15 m thickness) after 2 days of curing. The leveling pad was at 0.15 m depth below the excavated ground. The wall face was made of segmental concrete panels (1.50 x 1.50 x 0.14 m^3). In this construction, 4 facing panels were installed in the middle zone of the wall width (9 x 6 x 6 m^3) with 8 reinforcement levels. The longitudinal members for all layers were 12 mm diameter and 4.2 m long. The transverse members were equal steel angles with 25 mm leg length (B) and 180 mm length (L). The transverse member spacing was 750 mm for all transverse members. The vertical spacing between each reinforcement level was 750 mm. The horizontal spacing was 750 mm for levels 4 to 8 and 0.50 for levels 1 to 3. The details of the bearing reinforcement for each layer are summarized in Table 1. The backfill was compacted in layers of approximately 0.15 m thickness to a dry density of about 90% the standard Proctor density. The compaction was carried out with a hand compactor. The degree of compaction and water content were checked regularly at several points for all the compaction layers by the sand cone method. Construction sequence is illustrated in Figure 5. The total time spent for the construction was 20 days. At 47 days after the completion of construction, the top of the embankment was raised by 1.2 m as additional surcharge to simulate the surcharge load of about 20 kPa.

Figure 3: Schematic diagram of the test wall with instrumentation

Figure 4: Full-scale test BRE wall.

Figure 5: Construction sequence of BRE wall.

Table 1: Reinforcement details for the test BRE wall (Horpibulsuk and Niramitkornburee, 2010).

2.3 Instrumentation Program

The BRE wall was extensively instrumented both in the subsoil foundation and within the wall itself. The ground water table observation well and piezometer were not used in this investigation because the ground water was deeper than 8 m depth (end of boring). The settlement plates were installed in the subsoil foundation and backfill. The earth pressure cells were installed in the subsoil and facing panels. Lateral movements of each segmental panel during construction were recorded by a theodolite with reference to the benchmark. Lateral movements after the end of construction were measured using digital inclinometers. The inclinometer casing was installed from top of wall down to the medium dense sand about 4 m below the wall base. The strains and tensile forces along the longitudinal members were measured using waterproof type strain gauges. The measurement points were located at 0.23, 1.02, 1.81, 2.60 and 3.39 m from the wall. The strain gauges were installed at all eight layers of the bearing reinforcement in the middle zone of the wall.

3. MODEL PARAMETERS

The bearing reinforcement earth wall was modeled as a plane strain problem. The finite element mesh and boundary condition are shown in Fig. 6. The finite element mesh involved 15-node triangular elements for the backfill and the foundation. The nodal points at the bottom boundary were fixed in both directions and those on the side boundaries were fixed only in the horizontal direction. The simulation was performed in drained condition because the groundwater was not detected during the study. The model parameters related to

the compressibility were obtained from the conventional laboratory test that did not consider the time dependent behavior such as creep. The creep model is not within the scope of this study because this paper aims to simulate the wall behavior with the simple and well-known soil models for practical design.

Figure 6: Finite element model of BRE wall.

3.1 Backfill

The backfill was a clean sand, which consisted of 0.3% gravel, 97% sand and 2.7% silt. This sand was classified as poorly graded sand (SP), according to the Unified Soil Classification System (USCS). The backfill material was modeled as a linear elastic–perfectly plastic material with the Mohr–Coulomb failure criteria. The apparent cohesion and the friction angle were determined using a large direct shear apparatus with the diameter of 35 cm and they are $c' = 0$ and $\phi' = 40$ degrees. This high friction angle (greater than 36 degrees) is acceptable for MSE wall construction. Considering the average normal pressure at mid-height of the backfill (3 m high), the average normal pressure was calculated to be about 60 kPa. The input parameter of sand at the average normal pressure of 60 kPa was selected to represent the backfill material properties of the BRE wall. The material properties of the backfill used for the finite element simulation are shown in Table 2.

Table 2: Model parameters for backfill and subsoil.

3.2 Weathered crust

The weathered crust layer was classified as a silty clay. The water content was 12% and the dry unit weight, γ_d was 17 kN/m^3. The apparent cohesion and the friction angle were determined using drained direct shear tests and equal to c' = 20 kPa and ϕ' = 26 degrees. An elastic, perfectly plastic Mohr-Coulomb model was used to simulate the behavior of the weathered crust layer. The material properties of the weathered crust layer used for the finite element simulations are also shown in Table 2.

3.3 Medium to very dense sand

The medium to very dense sand layer was classified as clayey sand, according to the USCS. It consisted of 15-18% gravel, 48-60% sand, 8-10% silt and 16-23% clay. The natural water content was 12-20% and the dry unit weight, $\gamma_{d,\max}$ was 17-19 kN/m^3. Based on a drained direct shear test, the strength parameters were c' = 0 and ϕ' = 37 degrees. This is typical of the residual soil in the SUT campus (Horpibulsuk et al., 2008). An elastic, perfectly plastic Mohr-Coulomb model was used to simulate the behavior of this medium to very dense sand. The material properties used for the finite element simulations are shown in Table 2.

3.4 Soil-reinforcement interface parameter

The geotextile elements, which cannot resist the bending moment, were employed to model the bearing reinforcement, even though it is composed of longitudinal and transverse members. This modeling converts the contribution of both the friction and bearing resistances to the equivalent friction resistance. The equivalent friction resistance is represented by the interface factor, R. The input parameter for this element is an axial stiffness, AE, where A is

the cross-sectional area of longitudinal member and E is the modulus of elasticity of the material (steel). The test longitudinal member was 12 mm diameter and 2.6 m length. The axial stiffness of bearing reinforcement used in laboratory model test is shown in Table 3. The width of the transverse member in the laboratory model test was 0.15 m. The soil/bearing reinforcement interface parameter, R, was from the back analysis of the laboratory pullout tests by Horpibulsuk and Neramitkornburee (2010) (Figure 7). The elastic perfectly-plastic model was used to simulate the constitutive relation of the interface between soil and bearing reinforcement. There was no evidence of the bending of the transverse members from the retrieved bearing reinforcements, which indicates that the deformation of the transverse members during pullout was in the elastic range with a very small magnitude. It is thus assumed that the transverse members are rigid. Consequently, the pullout displacement and pullout force mobilized insignificantly varies over the length of the reinforcement and the R value is dependent on only the numbers of transverse member, n. As n increases, the R value increases (stiffness increases). The n = 2 and 3 were considered to determine the R that are the same as the full-scale BRE wall. The laboratory pullout test was modeled as a plane strain problem. The nodal points at the bottom boundary were fixed in both directions and those on the side boundaries were fixed only in the horizontal direction. The finite element mesh was comprised of 15-nodes triangular elements. The finite element mesh consisted of 558 triangular soil elements not including interface elements. The parameters for bearing reinforcement used in the BRE wall model test are tabulated in Table 4.

Figure 7: Finite element model of pullout tests.

Table 3: Model parameters for the bearing reinforcement in laboratory pullout test.

Table 4: Model parameters for reinforced element structure.

3.5 Facing concrete panels

The wall face was made of segmental concrete panel, which measured 1.50 x 1.50 x 0.14 m in dimension. The facing panel was modeled as a beam element. The values for the strength parameters and the modulus of elasticity are shown in Table 4. The soil-facing panel interface, *R*, was taken as 0.9, which is generally used for concrete panels (Bathurst, 1993).

4. FINITE ELEMENT ANALYSES

4.1 Soil-reinforcement interface coefficient, *R*

Figures 8 and 9 show the measured and simulated total pullout force and displacement relationship of the 2.6 m length bearing reinforcements with 2 and 3 transverse members (n = 2 and 3), respectively. The test results within a small displacement of less than 5 mm were used to determine the interface coefficient, *R* which is consistent with the field wall movement. The small lateral wall movement was observed due to the base restriction effect of the hard stratum (Rowe and Ho, 1997). The interface coefficient, *R*, was derived by a back analysis varied until the modeled curves coincided with the laboratory curves. The *R* values of 0.65 and 0.75 provide the best simulation for 2 and 3 transverse members, respectively. These values were used for simulating the field performance of the BRE wall. This method of determining, *R* is analogous to that suggested by Bergado et al., (2003); and Khedkar and Mandal (2007 and 2009) for hexagonal wire mesh and cellular reinforcement.

Figure 8: Comparison between the simulated and measured pullout test result of the bearing reinforcement with two transverse members.

Figure 9: Comparison between the simulated and measured pullout test result of the bearing reinforcement with three transverse members.

4.2 Bearing stress

Figure 10 shows the relationship between bearing stress and construction time in both reinforced (0.5 and 2.4 m from wall facing) and unreinforced (4.5 m from facing) zones. The bearing stresses increased during construction due to the backfill placement. The bearing stress changed insignificantly with time after the completion of construction. The simulated bearing stresses for both front and back are very good in agreement with the measured ones. At 2.4 m away from the wall face, the bearing stresses during 10 days (1^{st} and 2^{nd} loading) of construction are very close to the measured ones but after the 2^{nd} loading, the simulated bearing stress is lower than the measured one, and hence the simulated final bearing stress is lower. The difference between the simulated and measured bearing stress might be due to the non-uniformity of compaction at this particular location; therefore, the earth pressure cell sank into the ground at about 32 kPa vertical pressure (2^{nd} loading). The bearing stress could be again recorded after the 3^{rd} loading that the earth pressure cell located on the hard compacted foundation. Figure 11 shows the measured and the simulated distribution of bearing stresses at the end of construction from the front to back. The simulated and measured bearing stresses patterns are in good agreement. Within the reinforced zone, the bearing stress distributes approximately in trapezoid shape, which is normally observed for embankments constructed on rigid foundation. The simulated bearing stress in the reinforced zone decreases from the front to back because the BRE wall behaves as a rigid body, retaining the unreinforced backfill. The maximum bearing stress at front is thus due to a eccentric load caused by the lateral thrust from the unreinforced backfill and the vertical load from the weight of segmental panels. The bearing stress insignificantly changes with distance in the unreinforced zone and being equal to that at the end of bearing reinforcement.

Figure 10: Comparison between the simulated and measured bearing stress change with construction time.

Figure 11: Comparison between the simulated and measured bearing stress distribution.

4.3 Settlement

The measured and simulated settlements of the BRE wall are illustrated in Figures 12 and 13. The observed data from the four settlement plates at the center of the BRE wall were compared with the simulation. The settlement increased with construction time (Figures 12). Because the wall was founded on the relatively dry and hard stratum, the immediate settlement was dominant (insignificant consolidation settlement). The simulated settlements during construction are very close to the measured ones. The simulated settlements decrease from front that is close to the facing panel (82 mm) to back (77 mm) (*vide* Figure 13). Even though the BRE wall behaves as a rigid block, which causes the large bearing stress at front (due to eccentric load), the settlement is almost uniform due to the contribution of the stiffness of the foundation and the reinforcements. Among the four measuring points, 2 measured data divert from the simulation results: at 0.8 m and 5 m (unreinforced zone) from the facing. The measured settlement at 0.8 m from the facing is slightly higher than the simulated one possibly because the foundation might be disturbed during the foundation excavation for making the leveling pad. The measured settlement in unreinforced zone (5 m from facing) is higher than the simulated one because the stiffness of the foundation in the unreinforced zone is lower than that in the reinforced zone (the foundation in the reinforced zone was compacted before constructing the BRE wall). In this simulation, the same modulus

of elasticity, *E* was applied to both unreinforced and reinforced zones for simplicity. A better simulation could be found if different *E* is used for the simulation. Overall speaking, the computed settlements in the reinforced zone from the FEM analysis agree reasonably well with the measured ones.

Figure 12: Comparison between the simulated and measured settlement change with construction time.

Figure 13: Comparison between the measured and computed settlements.

4.4 Lateral movement

The simulated and measured lateral movements are compared and shown in Figure 14. The measured lateral movement was the sum of the lateral movements during construction (measured by a theodolite) and after end construction (measured by digital inclinometers). The measured lateral movement is lower than the simulated one because the stiffness of the inclinometer casing prevents the soil lateral movement and the inclinometer casing was installed close to the leveling pad, which obstructs the movement of the inclinometer. However, based on the *R* values obtained from the back analysis of the laboratory pullout tests, the patterns of the lateral movement from both the simulation and measurement are almost the same. Lateral movement is caused by the wall settlement and pullout displacement of the reinforcement, which is governed by the *R* value. The *R* value also controls the tension in the reinforcement. The lower the *R* value, the greater the lateral movement and the lower the tension in reinforcement. The *R* values obtained from the back analysis are considered as suitable for simulating the field performance of the BRE wall because both the simulated lateral movement and the simulated tension in the reinforcement

(presented in the following section) are in good agreement with the measured ones. The simulated maximum lateral movement in the subsoil occurs between 0.5-1.5 m depth below original ground surface corresponding to the weathered crust. The simulated maximum wall movement occurs at about the mid-height with a small magnitude of 23.5 mm. Although the BRE wall rotated about the toe, at a certain stage of deformation process, a crack developed at about the middle of the wall height and the wall started to deform as two rigid panels with a progressive opening of the crack. This finding is in agreement with that by Pinto and Cousens (1996 and 2000).

Figure 14: Comparison between the simulated and measured lateral movements.

4.5 Lateral earth pressure

The simulated and measured lateral earth pressures during construction at wall face are depicted in Figure 15. The lateral earth pressures at wall facing panels were measured from earth pressure cells attached to the wall facing panels. The lateral earth pressure, σ_h at the wall facing panels is useful for designing the tie points and facing panels. The simulated lateral earth pressure increased during construction due to backfill placement. The simulated lateral earth pressures during construction are close to the measured ones for the three measurement points (0.375, 3.0 and 4.5 m from the wall base). The lateral earth pressures, σ_h are initially close to the at-rest value, $K_0\sigma_v$ where K_0 is the coefficient of at rest lateral earth pressure and σ_v is the vertical stress. With an increase in the backfill load, the lateral earth pressures, σ_h reduce and tend to approach the active value, $K_a\sigma_v$. Both K_0 and K_a were calculated from the Rankine's theory that the friction between wall and soil is ignored. At

0.375 m, the simulated σ_h is lower than the calculated $K_a \sigma_v$ due to the effect of the soil/wall interface. This finding is confirmed by Rowe and Ho (1997).

Figure 15: Comparison between the simulated and measured lateral earth pressures at different depths and applied vertical stresses.

4.6 Tensions in the bearing reinforcement

The simulated and measured tensions during construction at the points 0.23, 1.81 m distance from the wall face are shown in Figure 16. The simulated tension forces are in good agreement with the measured ones. The tension forces for both points increased with the vertical stress. Figure 17 shows the comparison between the simulated and the measured tension forces in the bearing reinforcements at 14 days after the completion of construction and 10 days after additional surcharge load 20 kPa. The smooth relationships between tension and distance are found for both the measured data and simulation results. The smooth curves (without sharp peaks) from the measured data are because all the strain gauges were attached to the longitudinal members (no strain gauge was on the transverse members) and the stresses in the transverse members might be insignificant or the strains in the steel might be too small. The possible failure plane recommended by AASHTO (2002) for inextensible reinforcements is also shown in the figure by a dash line. Most of the simulated maximum tension forces lie on the recommended possible failure plane. In practice, the maximum tension (possible failure) plane recommended by AASHTO (2002) can be thus used to examine the internal stability of the BRE wall using the limit equilibrium analysis. This simulated maximum tension pattern is approximate bi-linear and similar to the previous studies for different types of reinforcement (Chai, 1992; Bergado et al., 1995; Alfaro et al., 1997; and Bergado and

Teerawattanasuk, 2007). This approximate bi-linear maximum tension plane is caused by the lateral movement of two facing panels at about the mid-height of the wall.

Figure 16: Comparison between the simulated and measured tension forces for different reinforcement layers and applied vertical stresses at 0.23 and 1.81 m from the wall face.

Figure 17: Comparison between the simulated and measured tension forces in the reinforcements.

---

5. CONCLUSIONS

This paper presents a numerical analysis of the bearing reinforcement earth (BRE) wall constructed on the hard stratum by PLAXIS 2D. The goetextile elements, which cannot resist the bending moment, were used to model the bearing reinforcements by converting the contribution of both the friction and bearing resistances to the equivalent friction resistance. This modeling is considered to be applicable and practical for working state (small pullout displacement). The equivalent friction resistance is represented by the interface factor, R, which was determined from the back analysis of the laboratory pullout test. The R values of 0.65 and 0.75 were obtained for the bearing reinforcements with 2 and 3 transverse members, respectively. The BRE wall was modeled under a plane strain condition and the reinforcements were modeled using geotextile elements, which cannot resist the bending moment. Overall, the behavior of the BRE wall is simulated satisfactorily and agreed well with the predictions. The changes in foundation settlements, bearing stresses, lateral earth pressures and tensions in the reinforcements during and after construction are in good agreement with the measured ones. The bearing stress distribution is approximately trapezoid

shape as generally observed for embankments found on hard stratum. The foundation settlement is almost uniform due to the effect of high stiffness of the foundation and reinforcements. The simulated lateral earth pressures for different depths are initially close to the at-rest Rankine lateral earth pressure. During construction, the simulated lateral earth pressures approach the active Rankine lateral earth pressure and are lower than the active Rankine lateral earth pressure especially at about wall base because of the effect of the wall/soil interface. The simulated maximum lateral wall movement occurs at about the mid-height. Although the BRE wall rotates about the toe, at a certain stage of deformation process, a crack develops at the middle of the wall height and the wall starts to deform as two rigid blocks with a progressive opening of the crack. This results in the approximate bilinear maximum tension (possible failure) plane. This maximum tension (possible failure) plane is very close to that recommended by AASHTO (2002) for inextensible reinforcements. In practice, this recommended maximum tension plane is acceptable to examine the internal stability of the BRE wall. The simulation approach presented was successfully applied to investigate the performance of the BRE wall in Thailand.

ACKNOWLEDGEMENTS

The first author is grateful to the Thailand Research Fund for Ph.D. study financial support under the Ph.D. Royal Jubilee program. Financial support, facilities and equipment provided from the Suranaree University of Technology are very much appreciated.

REFERENCES

AASHTO, 1996. Standard specifications for highway and bridge, first ed. American Association of State Highway and Transportation Officials, Washington D.C.

AASHTO, 2002. Standard specifications for highway and bridge, seventh ed. American Association of State Highway and Transportation Officials, Washington D.C.

Abdelouhab, A., Dias, D., Freitag, N., 2011. Numerical analysis of the behaviour of mechanically stabilized earth walls reinforced with different types of strips. Geotextiles and Geomembranes 29, 116-129.

Alforo, M.C., Hayashi, S., Miura, N., Bergado, D.T., 1997. Deformation of reinforced soil-embankment system on soft clay foundation. Soils and Foundations 37 (4), 33-46.

Al Hattamleh, O., Muhunthan, B., 2006. Numerical procedures for deformation calculations in the reinforced soil walls. Geotextitles and Geomembranes 24 (1), 52-57.

Bathurst, R.J., 1993. Investigation of footing resistant on stability of large-scale reinforced soil wall tests. Proceedings of 46th Canadian Geotechnical Conference.

Bergado, D.T., Chai, J.C., Miura, N., 1995. FE analysis of grid reinforced embankment system on soft Bangkok clay. Computers and Geotechnics 17, 447–471.

Bergado, D.T., Chai, J.C., Miura, N., 1996. Prediction of pullout resistance and pullout force-displacement relationship for inextensible grid reinforcements. Soils and Foundations 36 (4), 11-22.

Bergado, D.T., Teerawattanasuk, C., 2007. 2D and 3D numerical simulations of reinforced embankments on soft ground. Geotextiles and Geomembranes 26 (1), 39–55.

Bergado, D.T., Teerawattanasuk, C., Youwai, S., Voottipruex, P., 2000. FE modeling of hexagonal wire reinforced embankment on soft clay. Canadian Geotechnical Journal 37 (6), 1–18.

Bergado, D.T., Youwai, S., Teerawattanasuk, C., Visudmedanukul, P., 2003. The interaction mechanism and behavior of hexagonal wire mesh reinforced embankment with silty sand backfill on soft clay. Computers and Geotechnics 30, 517–534.

Chai, J.C., 1992. Interaction between Grid Reinforcement and Cohesive-Frictional Soil and Performance of Reinforced Wall/Embankment on Soft Ground, D.Eng. Dissertation, Asian Institute of Technology, Bangkok, Thailand.

Hatami, K., Bathurst, R.J., 2005. Development and verification of numerical model for the analysis of geosynthetic-reinforcement soil segmental wall under working stress condition. Canadian Geotechnical Journal 42, 1066-1085.

Hatami, K., Bathurst, R.J., 2006. Numerical model for the analysis of geosynthetic-reinforced soil segmental wall under surcharge loading. Journal of Geotechnical and Geoenvironmental Engineering 136 (6), 673-684.

Horpibulsuk, S., Niramitkornburee, A., 2010. Pullout resistance of bearing reinforcement embedded in sand. Soils and Foundations 50 (2), 215-226.

Horpibulsuk, S., Kumpala, A., Katkan, W., 2008. A case history on underpinning for a distressed building on hard residual soil underneath non-uniform loose sand. Soils and Foundations 48 (2), 267-286.

Horpibulsuk, S., Suksiripattanapong, C., Niramitkornburee, A., 2010. A method of examining internal stability of the bearing reinforcement earth (BRE) wall. Suranaree Journal of Science and Technology 17 (1), 1-11.

Horpibulsuk, S., Suksiripattanapong, C., Niramitkornburee, A., Chinkulkijniwat, A., Tangsuttinon, T., 2011. Performance of earth wall stabilized with bearing reinforcements. Geotextiles and Geomembranes 29 (5), 514-524.

Hufenus, R., Rueegger, R., Banjac, R., Mayor, P., Springman, S. M., Bronnimann, R., 2006. Full-scale field tests on geosynthetic reinforced unpaved roads on soft subgrade. Geotextiles and Geomembranes 24 (1), 21-37.

Khedkar, M.S., Mandal, J.N., 2007. Pullout response study for cellular reinforcement. In: Proceedings of Fifth International Symposium on Earth Reinforcement, IS Kyushu ’07, November 14–16, 2007, Fukuoka, Japan, pp. 293–298.

Khedkar, M.S., Mandal, J.N., 2009. Pullout behavior of cellular reinforcements. Geotextiles and Geomembranes 27 (4), 262-271.

McGown, A., Andrawes, K.Z., Pradhan, S., Khan, A.J., 1998. Limit state analysis of geosynthetics reinforced soil structures. Keynote lecture. In: Proceedings of 6th International Conference on Geosynthetics, March, 25-29, 1998, Atlanta, GA, USA, pp. 143-179.

Park, T., Tan, S.A., 2005. Enhanced performance of reinforced soil walls by the inclusion of short fiber. Geotextiles and Geomembranes 23 (4), 348-361.

Pinto, M.I.M., Cousens, T.W., 1996. Geotextile reinforced brick faced retaining walls. Geotextiles and Geomembranes 14 (9), 449-464.

Pinto, M.I.M., Cousens, T.W., 2000. Effect of the foundation quality on a geotextile-reinforced brick-faced soil retaining wall. Geosynthetics International 7 (3), 217-242.

Rowe, R.K., Ho, S.K., 1995. Continuous panel reinforced soil walls on rigid foundations. Journal of Geotechnical and Geoenvironmental Engineering 123 (10), 912-920.

Skinner, G.D., Rowe, R.K., 2005. Design and behavior of a geosynthetic reinforced retaining wall and bridge abutment on a yielding foundation. Geotextitles and Geomembranes 23 (3), 234-260.

Figure Caption

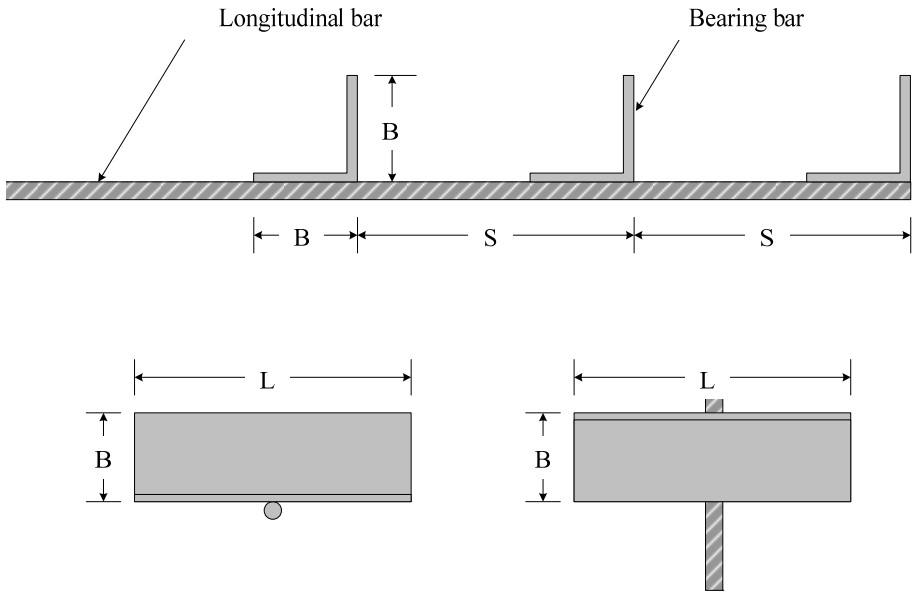

Figure 1: Configuration of the bearing reinforcement (Horpibulsuk and Niramitkornburee, 2010).

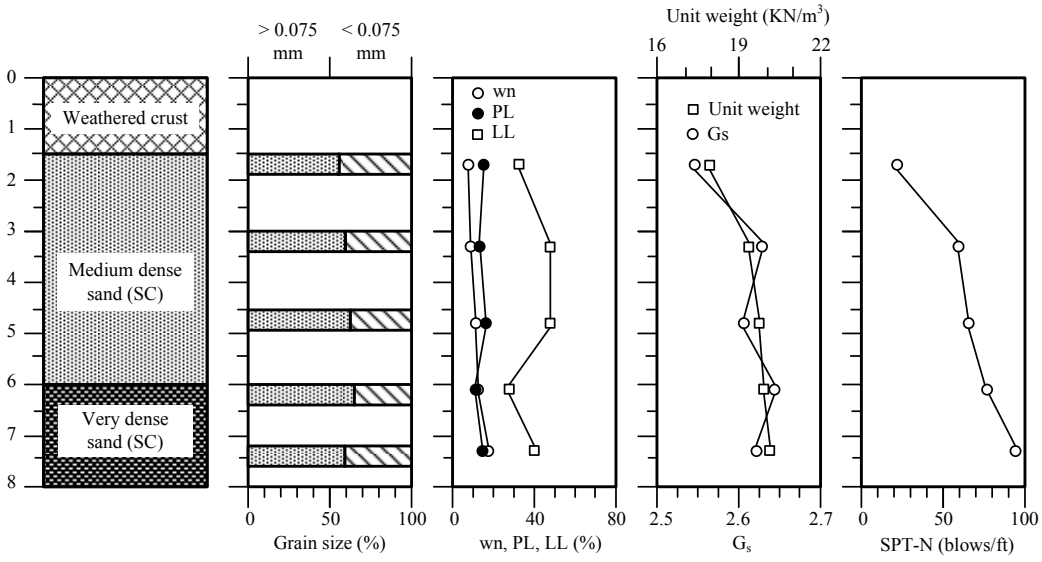

Figure 2: General soil profile.

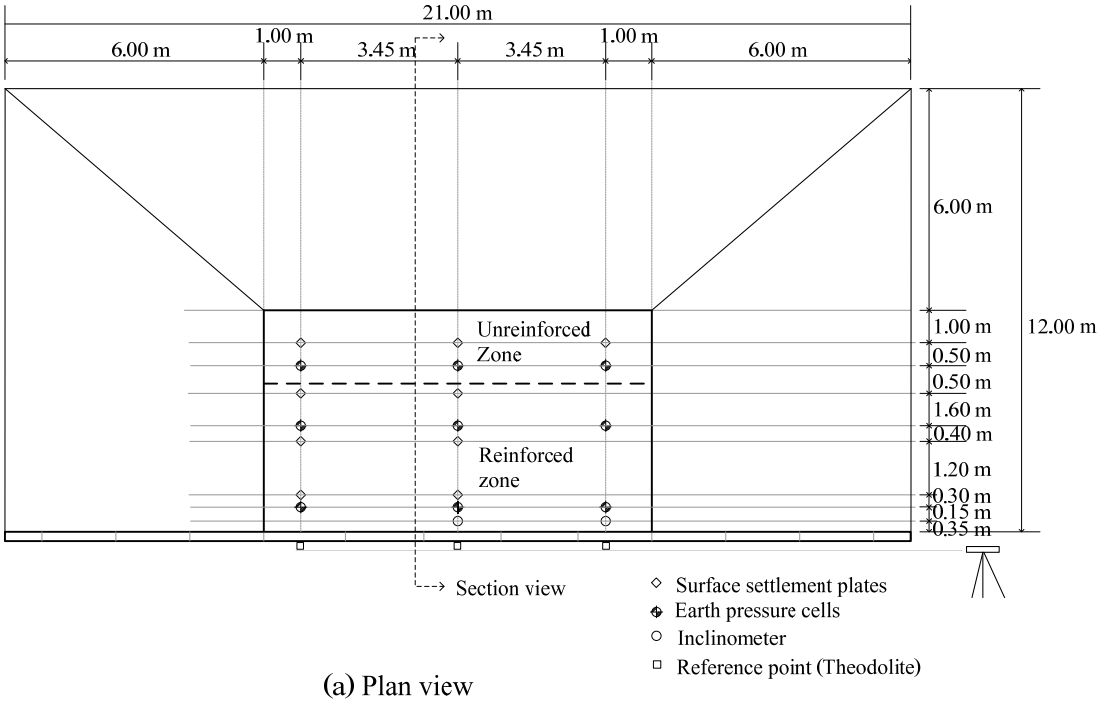

(a) Plan view

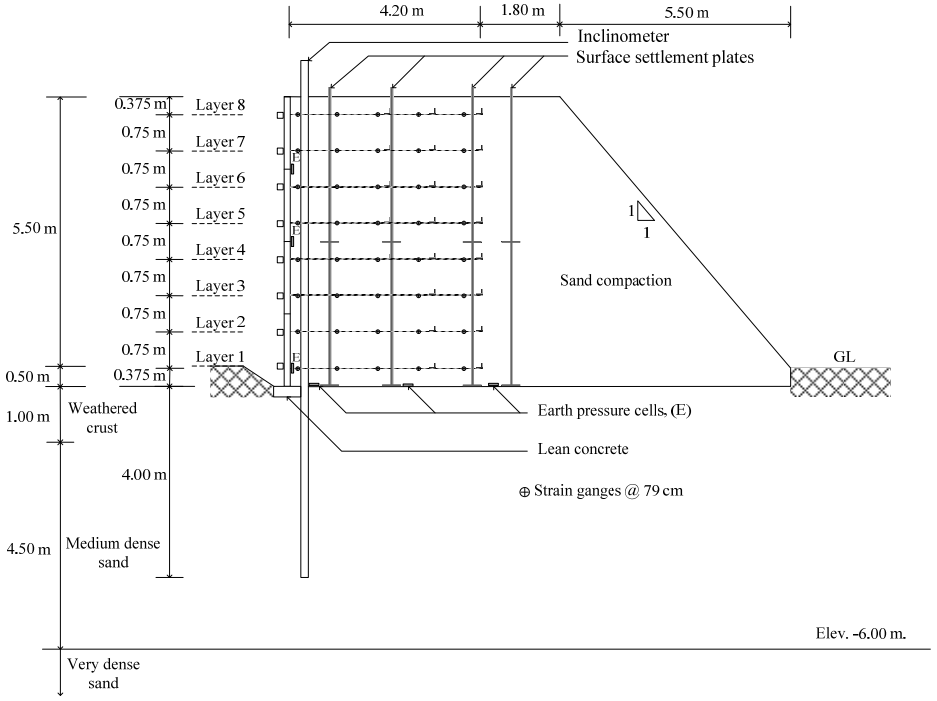

(b) Section view

Figure 3: Schematic diagram of the test wall with instrumentation.

Figure 4: Full-scale test BRE wall.

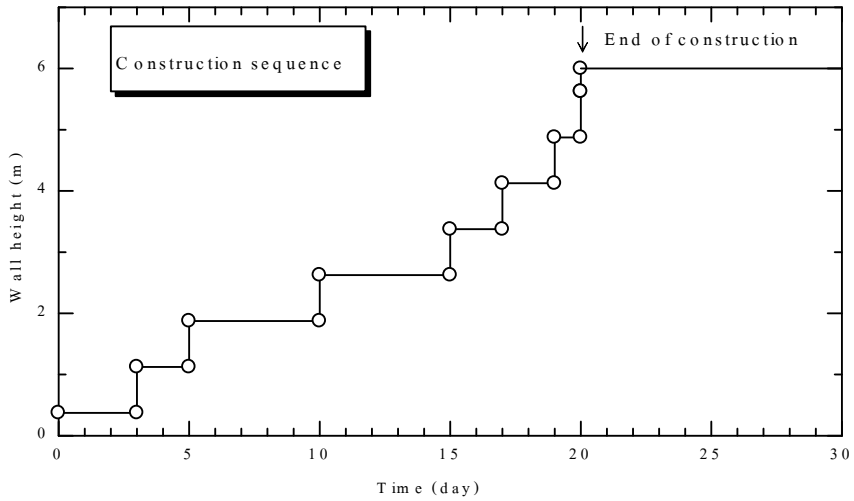

Figure 5: Construction sequence of BRE wall.

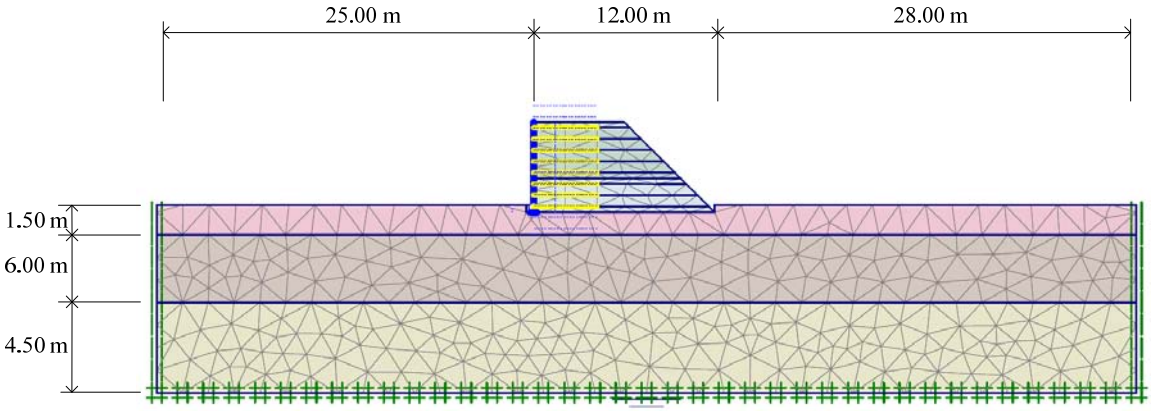

Figure 6: Finite element model of BRE wall.

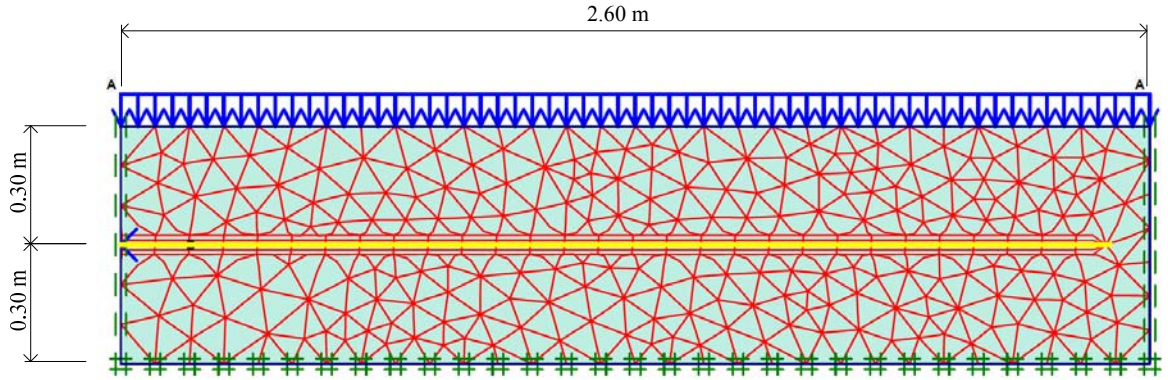

Figure 7: Finite element model for pullout tests.

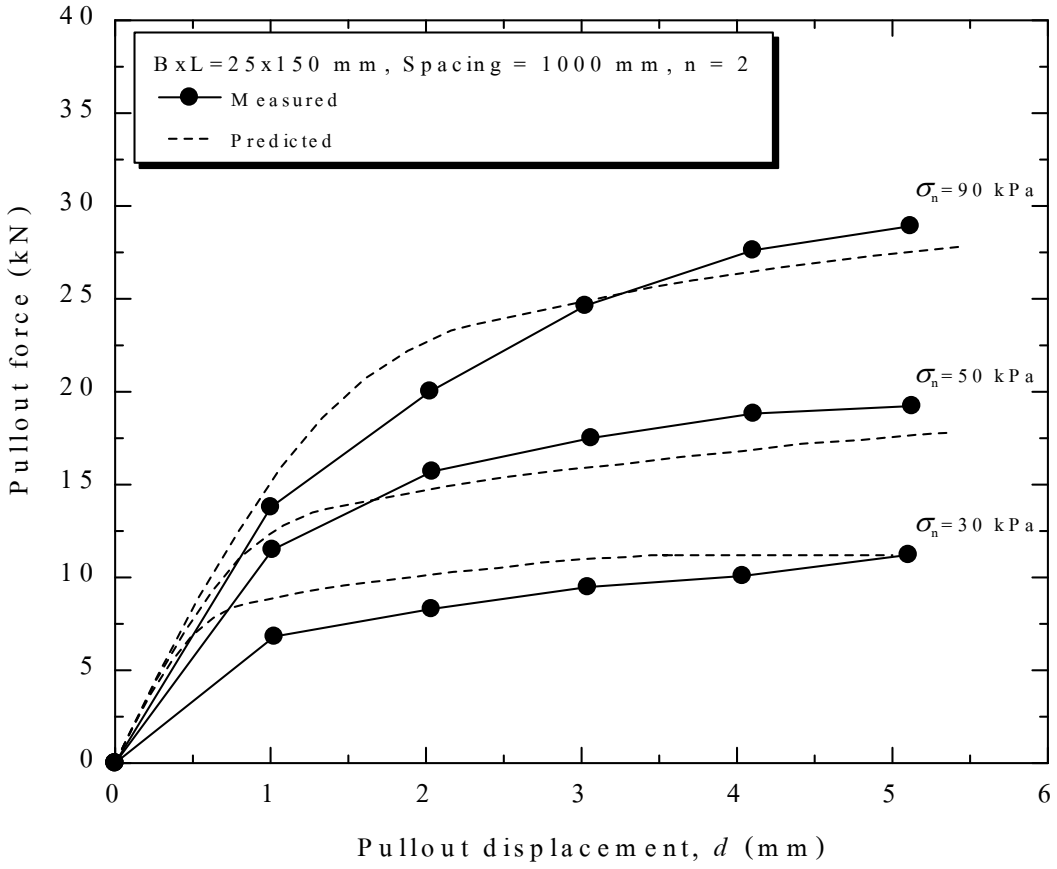

Figure 8: Comparison between the simulated and measured pullout test result of the bearing reinforcement with two transverse members.

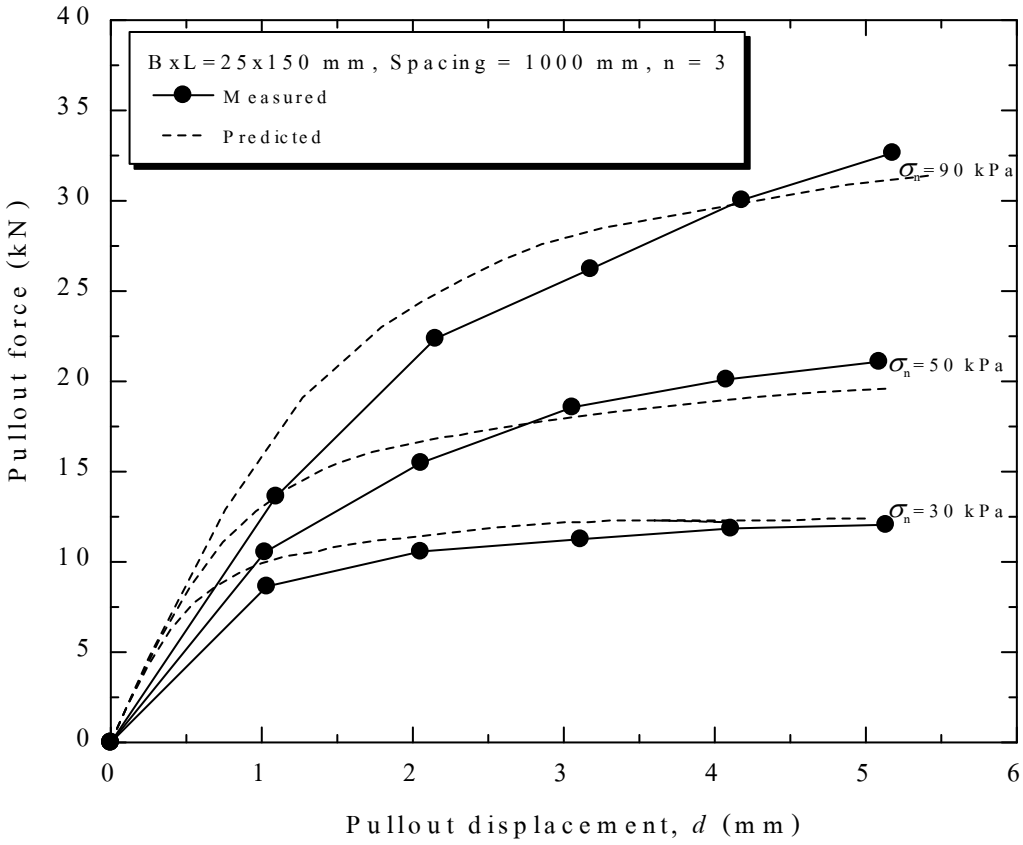

Figure 9: Comparison between the simulated and measured pullout test result of the bearing reinforcement with three transverse members.

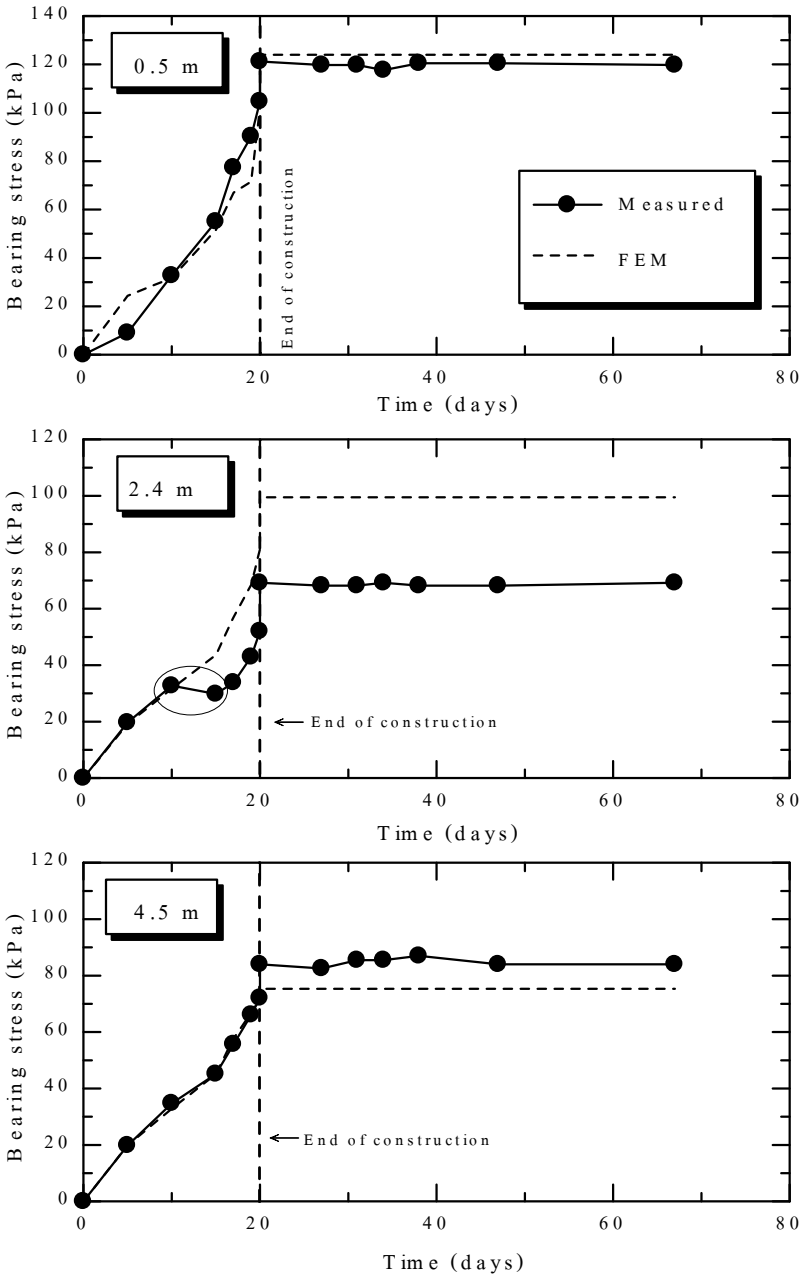

Figure 10: Comparison between the simulated and measured bearing stress change with construction time.

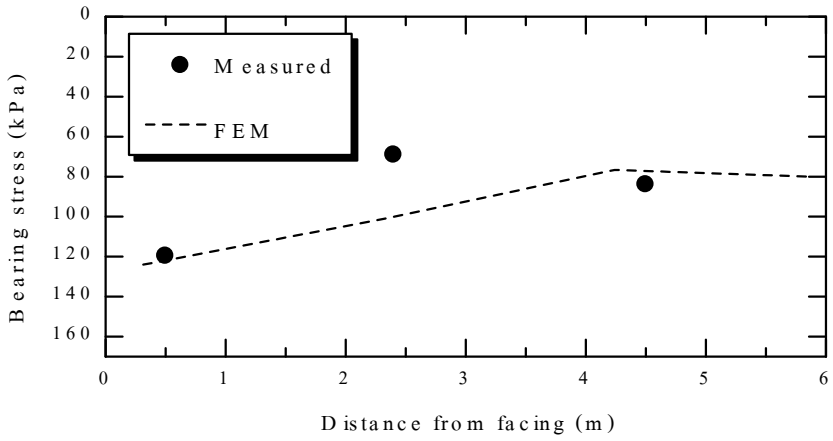

Figure 11: Comparison between the simulated and measured bearing stress distribution.

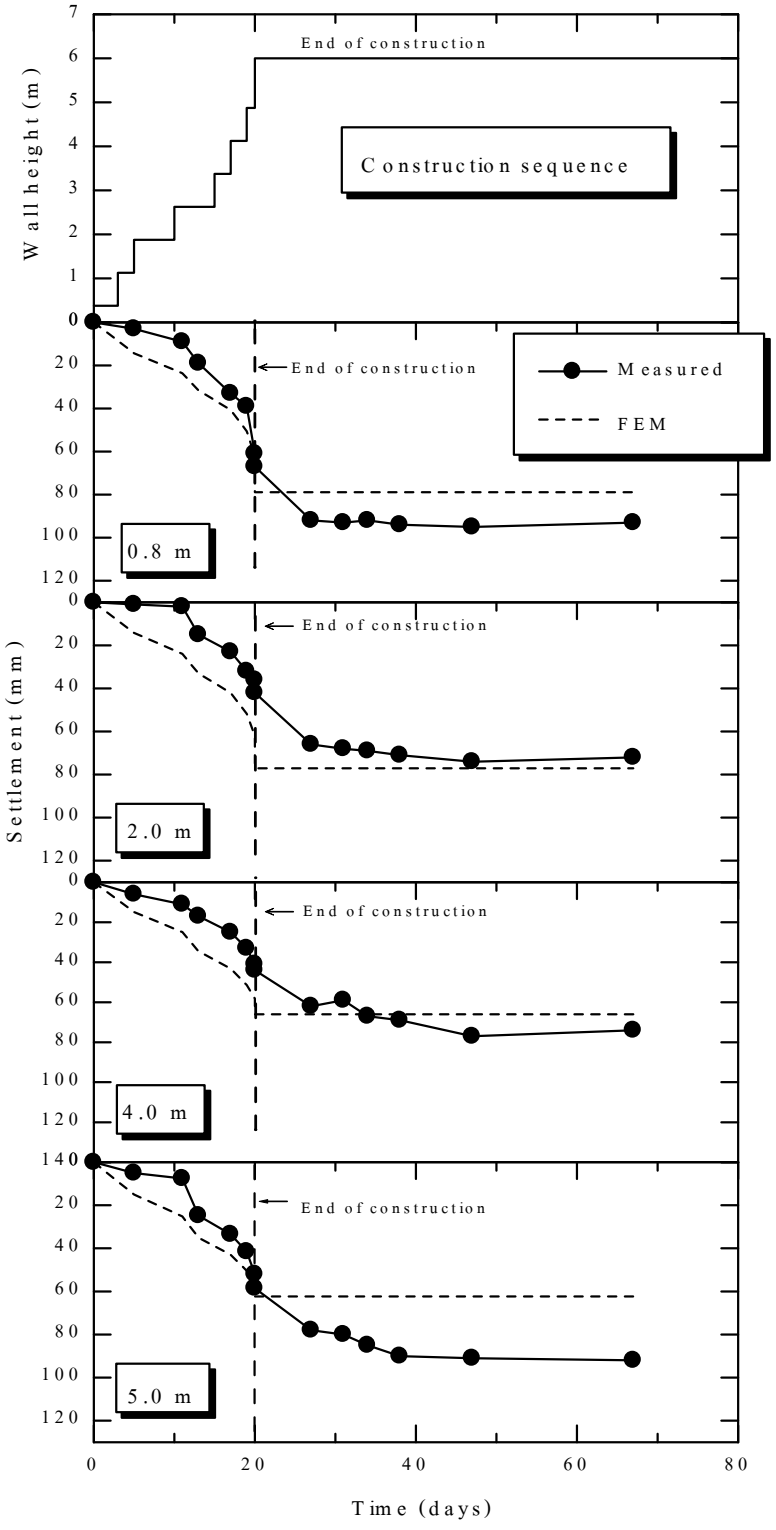

Figure 12: Comparison between the simulated and measured settlement change with construction time.

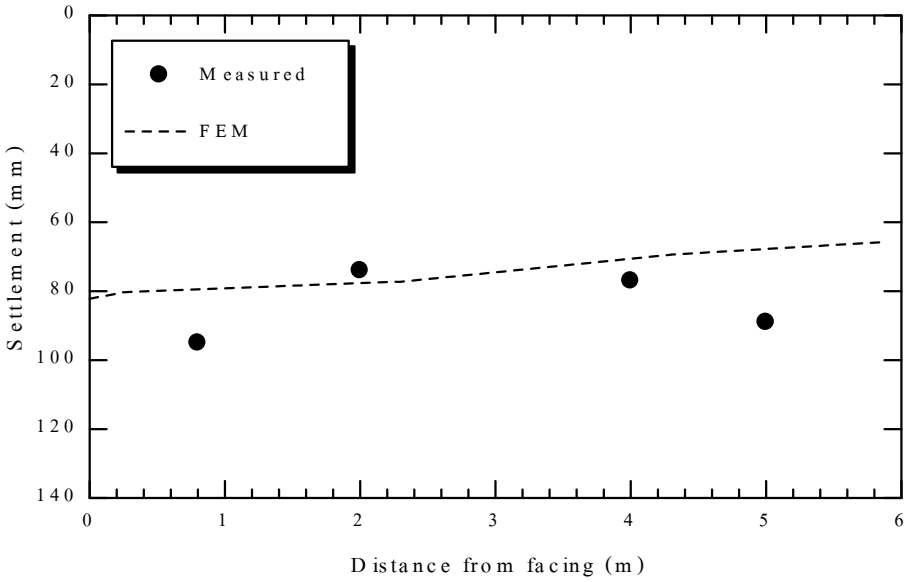

Figure 13: Comparison between the measured and computed settlements.

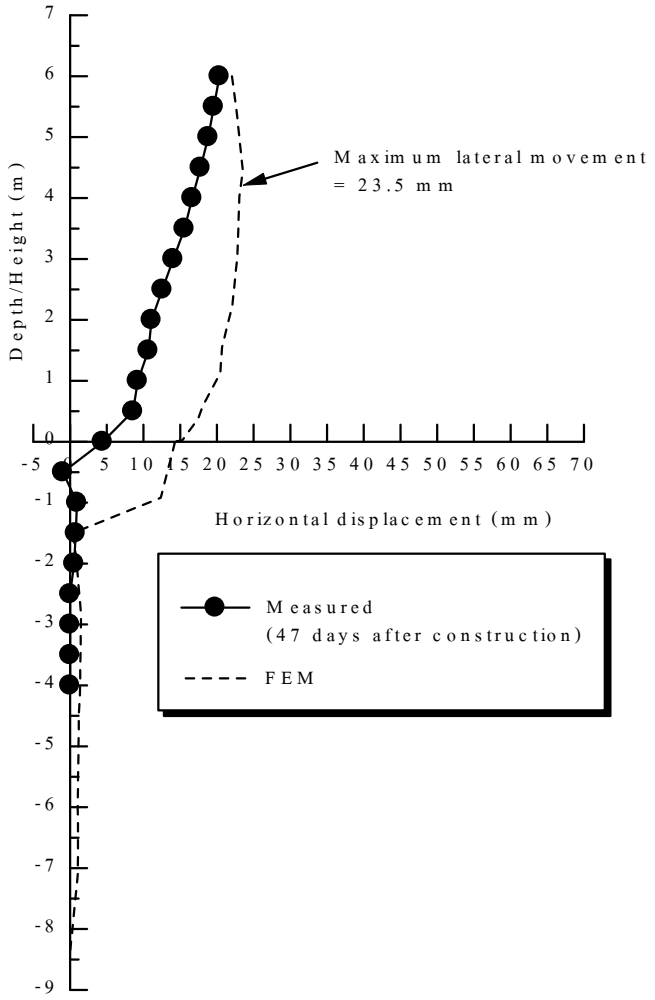

Figure 14: Comparison between the simulated and measured lateral movements.

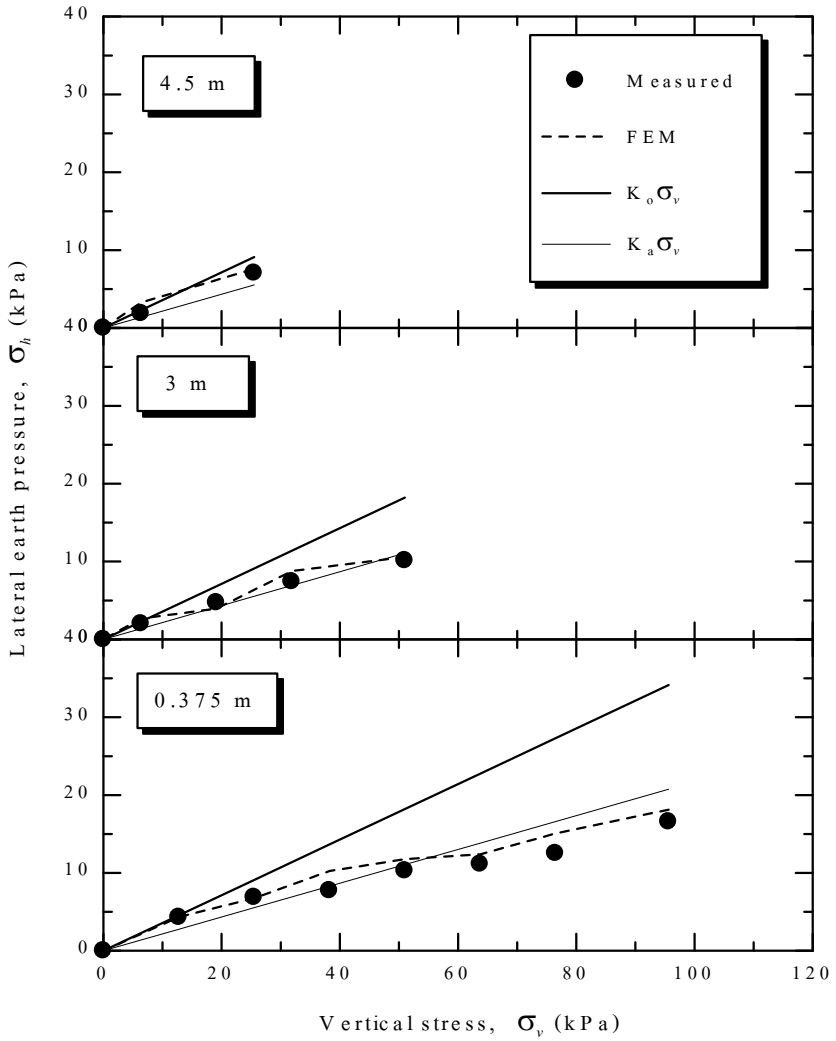

Figure 15: Comparison between the simulated and measured lateral earth pressures at different depths and applied vertical stresses.

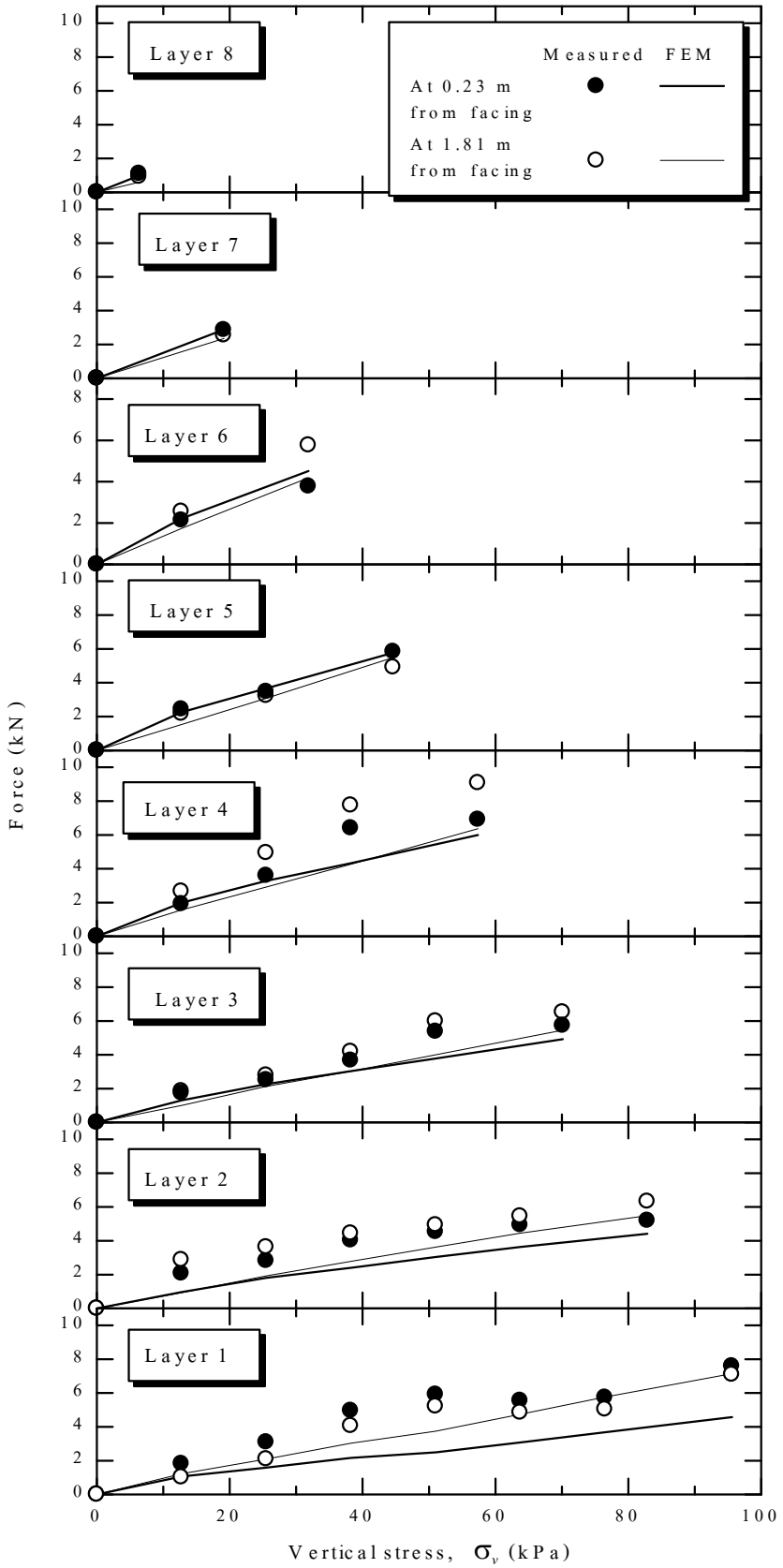

Figure 16: Comparison between the simulated and measured tension forces for different reinforcement layers and applied vertical stresses at 0.23 and 1.81 m from the wall face.

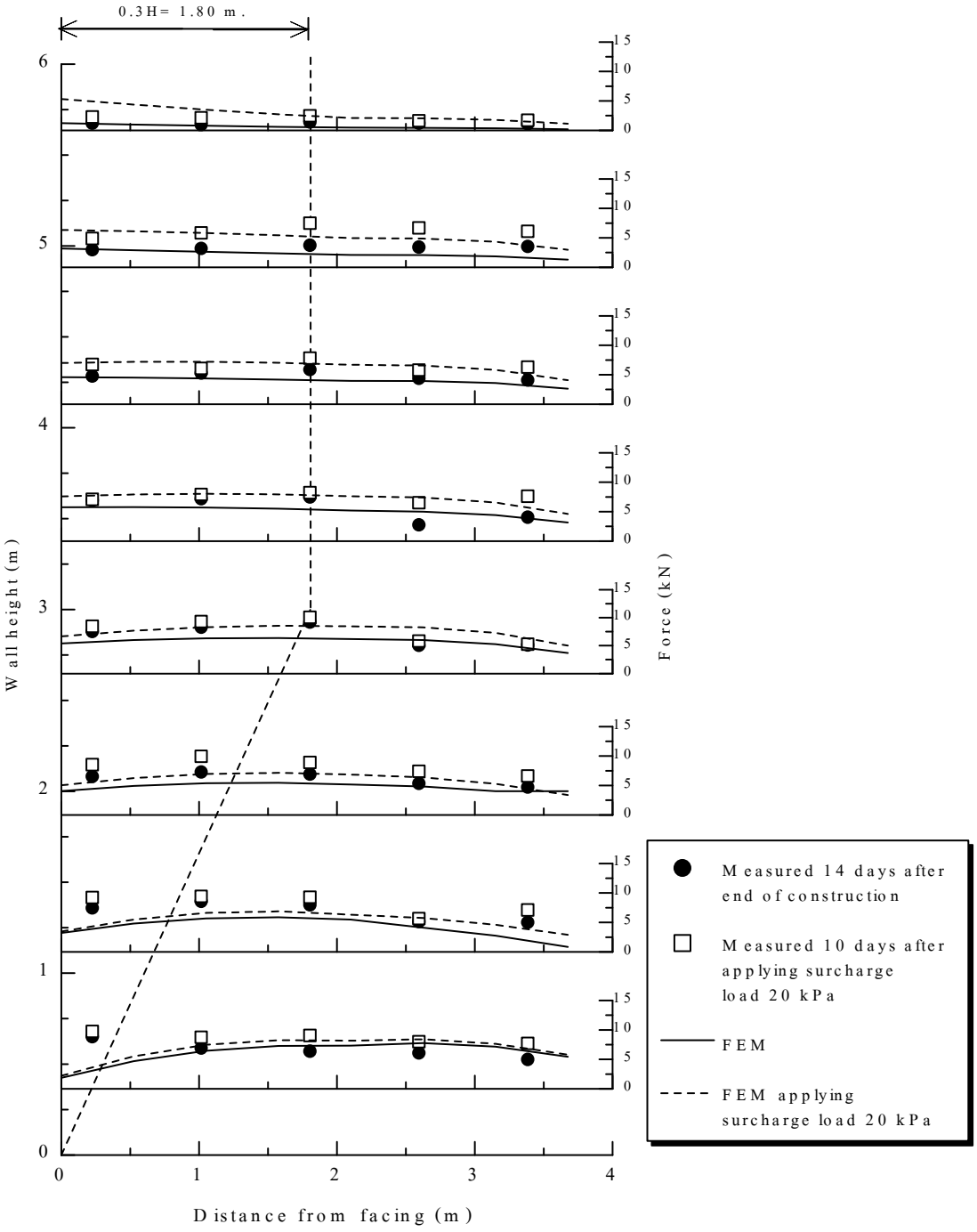

Figure 17: Comparison between the simulated and measured tension forces in the reinforcements.

Table Caption

Table 1: Reinforcement details for the test BRE wall (Horpibulsuk and Niramitkornburee, 2010).

Table 2: Model parameters for backfill and subsoil.

Table 2: Model parameters for the bearing reinforcement in laboratory pullout test.

Table 3: Model parameters for reinforced element structure.

Table 1
Reinforcement details for the test wall (Horpibulsuk and Niramitkornburee, 2010).

Facing panel	Reinforcement layers	Spacing between longitudinal members (12 mm deformed bar)	Number of transverse members (25x25x3 mm equal angle)
1	1 (bottom)	500 mm	2
	2	500 mm	2
2	3	500 mm	2
	4	750 mm	3
3	5	750 mm	3
	6	750 mm	3
4	7	750 mm	3
	8 (Top)	750 mm	3

Table 2
Model parameters for backfill and subsoil.

Item	Backfill soil	Weathered crust	Medium dense sand	very dense sand
Material model	Mohr-Coulomb	Mohr-Coulomb	Mohr-Coulomb	Mohr-Coulomb
Material type	Drained	Drained	Drained	Drained
γ_{dry}	17 kN/m^3	17 kN/m^3	17.15 kN/m^3	18 kN/m^3
γ_{wet}	18.15 kN/m^3	18 kN/m^3	18.15 kN/m^3	19 kN/m^3
k_x	1 m/day	1 m/day	1 m/day	1 m/day
k_y	1 m/day	1 m/day	1 m/day	1 m/day
E_{ref}	35000 kN/m^2	1875 kN/m^2	40000 kN/m^2	50000 kN/m^2
ν'	0.33	0.30	0.25	0.25
c'	1	20 kPa	1	1
ϕ'	40^o	26^o	35^o	38^o
Ψ	8^o	0^o	3^o	8^o

Table 3
Model parameters for bearing reinforcement in laboratory model test.

Type	Modulus of elasticity (GPa)	Axial stiffness, EA (kN/m)
Bearing reinforcement	200	150796

Table 4
Model parameters for reinforced element structure.

Item	Bearing reinforcement	Facing concrete
Material model	Elastic	Elastic
EA	4.5E+4 kN/m	3.556E+6 kN/m
EI	-	5808 kNm^2/m
w	-	3.36 kN/m/m
ν'	-	0.15